



# DAMAGE ASSESSMENT OF A BUILDING UNDER AN EARTHQUAKE VIA THE TVARX MODEL AND BAYESIAN APPROACH

C. S. Huang<sup>(1)</sup>, C. Y. Liu<sup>(2)</sup>, W. C. Su<sup>(3)</sup>

<sup>(1)</sup> Professor, National Chiao Tung University, [cshuang@mail.nctu.edu.tw](mailto:cshuang@mail.nctu.edu.tw)

<sup>(2)</sup> Ph.D. Candidate, National Chiao Tung University, [sinrassis.cv97g@g2.nctu.edu.tw](mailto:sinrassis.cv97g@g2.nctu.edu.tw)

<sup>(3)</sup> Associate Research Fellow, National Center for High Performance Computing, [1203017@nchc.narl.org.tw](mailto:1203017@nchc.narl.org.tw)

## Abstract

The work proposes a procedure for the damage assessment of a building under a strong earthquake. The Cauchy wavelet transform is applied to the measured acceleration responses of a building and a time-varying autoregressive with exogenous input (TVARX) model with time-variant coefficients expanded as piecewise polynomial functions. The time-variant modal parameters of the building are directly identified from the coefficients of the appropriately established TVARX model. A Bayesian approach for dynamical model updating is employed to identify the variations of stiffness components with time using those identified time-varying modal parameters. Consequently, the damaged stories of the building are located and the severity of the damage can be determined. The proposed approach is validated through processing the numerically simulated acceleration responses of a six-story shear building with time varying stiffness and damping under base excitation with considering the effects of noise and incomplete measurement. Finally, the proposed approach is applied to handle the acceleration responses of a five-story steel frame in a shaking table test with a strong earthquake input. The frame is 3 m long, 2 m wide and 6.5 m high, and its columns of the first story yield during the test.

*Keywords:* Damage assessment; Building; TVARX model; Bayesian approach

## 1. Introduction

A structure may sustain damage either when subjected to severe loading, such as a strong earthquake, or when its material is degraded. The serviceability and safety of structures depend on the detection and location of structural damage. Early detection of structural degradation or damage is essential for preventing catastrophic failure. Research on structural health monitoring has been received more and more attention in civil engineering.

Vibration-based damage detection methods, which utilize the dynamic characteristics (modal frequencies, damping ratios, and mode shapes) of a structure, are simple and widely adopted [1-4]. The main idea behind these methods is that damage in a structure typically changes the stiffness and damping of the structure and results in changes in its dynamic characteristics. Friswell *et al.* [5], Messina *et al.* [6] and Zapico and González [7] presented various approaches employing the modal frequencies of full structures to detect damage. However, these methods are not very effective because modal frequencies mainly depend on the global behaviors of the structure, whereas damage is a rather local phenomenon. Some indexes based on mode shapes have been proposed; for instance, MAC (Modal Assurance Criterion) [8], COMAC (Coordinate Modal Assurance Criterion) [9], MSE (Modal Strain Energy) [10], EEQ (Elemental Energy Quotient) [11], and EMSEC (Elemental Modal Strain Energy Change) [12]. MAC and COMAC are easy to apply, but they are not very sensitive to the existence of damage. To estimate the MSE, EEQ and EMSEC for a damaged structure, the stiffness matrix of the structure in undamaged state, which is difficult to accurately determine, is needed. Pandey *et al.* [13] applied curvature mode shapes to locate damage in a beam, and Sampaio *et al.* [14] further proposed frequency response function curvature method and evaluated the efficiency of this method using numerically simulated data and experimental data for a real bridge. Using modal frequencies and mode shapes, Lin [15] and Pandey and Biswas [16] established flexibility matrices of a structure in undamaged and damaged states, and located damage by considering changes in the components of the flexibility matrices. To take account of only a very limited number of sensors in a structural health monitoring system, sub-structural identification techniques have also been proposed. Koh *et al.* [17] employed the extended Kalman filter along with a weighted global



iteration algorithm to determine the stiffness matrix and the damping matrix of a sub-structure, while Zhao *et al.* [18] estimated the stiffness matrix and the damping matrix of a sub-structure in the frequency domain using an iteration algorithm. Su *et al.* [19] developed a simple and efficient sub-structural approach to locate the stories whose properties (stiffness and mass) change in the life cycle of a shear building by using ARX model.

To assess damage in a structure, the aforementioned approaches deal with (equivalent) linear time invariant structures and require both the reference data (the data of structure without damage) and the data after damage. In practice, however, the reference data may not be available or difficult to establish because they are affected by environmental conditions such as temperature [20] and humidity [21], and after a severe event, such as a strong earthquake, it may not be feasible to conduct vibration tests to obtain meaningful data for damage identification. It would be desirable for a data analysis method to be capable of detecting the structural damage based solely on the vibration data measured during a severe event, such as a strong earthquake, without a prior knowledge of the undamaged structure.

To fulfil such need, the present work assumes that the mass matrix of a building is known and adapts a Bayesian probabilistic method [22], which is a model updating approach, to estimate instantaneous stiffness matrices of a building using the instantaneous natural frequencies and mode shapes of the structure. The damage in the building is further assessed from the changes in the instantaneous stiffness matrices at different time. The instantaneous natural frequencies and mode shapes are identified using the method recently developed by the authors [23], in which a time varying autoregressive with exogenous input (TVARX) model along with the Cauchy wavelet transform is used to establish an input-output relationship of the structure from its dynamic responses and input forces. The presented approach is validated using the numerically simulated earthquake acceleration responses of a six-story shear building, which has time dependent stiffness and damping in the first story. The incompletely measured noisy responses and input with 10% variances of the noise-to-signal ratio (NSR) are processed. For practical concerns, the bandwidth of the stiffness matrix to be identified is not assumed to be one, which is the bandwidth of the stiffness matrix for a shear building. Then, this procedure is further applied to the measured acceleration responses of a five-story steel frame in a shaking table test, to demonstrate the feasibility of applying the proposed procedure to real data. The columns in the first story of the steel frame were found to yield from the measured strains.

## 2. Methodology

A structure under damage typically shows nonlinear dynamical behaviors in which structural stiffness and damping are implicitly dependent on time. The time dependence of structural stiffness and damping in a damaged structure leads to the instantaneous modal parameters of the structure varying with time. Consequently, the procedure of the proposed approach is to identify instantaneous frequencies and mode shapes from an appropriate TVARX model, which is established from the measured acceleration responses of a building under an earthquake. The significant time dependence of instantaneous modal parameters of a building indicates that the building can be damaged during an earthquake. The stiffness matrices at different time are estimated from the identified instantaneous frequencies and mode shapes via a model updating technique. Comparisons of stiffness components at different time reveal the locations of damage and the severity of damage. Herein, the method of Huang *et al.* [23] is adapted to identify instantaneous frequencies and mode shapes of a building under an earthquake, and the approach of Yuen [22] is applied to construct the stiffness matrices of a building at different time from the identified instantaneous frequencies and mode shapes. Both methods are briefly introduced below.

### 2.1 Identification of instantaneous modal parameters

The mathematic expression for a TVARX model is

$$\mathbf{z}(t) = \sum_{i=1}^I \Phi_i(t-i)\mathbf{z}(t-i) + \sum_{j=0}^J \Theta_j(t-j)\bar{\mathbf{f}}(t-j) + \bar{\mathbf{a}}(t) \quad (1)$$



where  $\mathbf{z}(t) = (\mathbf{y}^T(t), \dot{\mathbf{y}}^T(t))^T$ ,  $\bar{\mathbf{f}}(t-j) = (\mathbf{f}^T(t-j), \mathbf{0}^T)^T$ ,  $\mathbf{y}(t-i)$  and  $\mathbf{f}(t-i)$  are the vectors of measured responses and input forces at time  $t-i\Delta t$ , respectively;  $1/\Delta t$  is the sampling rate of the measurement,  $\Phi_i(t)$  and  $\Theta_j(t)$  are matrices of coefficient functions to be determined in the model, and  $\bar{\mathbf{a}}(t)$  is a vector representing the residual error accommodating the effects of measurement noise, modeling errors and unmeasured disturbances. It is well-known that Eq.(1) is equivalent to a discrete form of equations of motion when  $\bar{\mathbf{a}}(t)$  is absent. Huang *et al.* [24] showed that the measured displacement responses used for  $\mathbf{y}(t-i)$  ensure that the instantaneous modal parameters are directly identifiable from  $\Phi_i(t)$  without systematic errors.

Piecewise second-order polynomials are applied to expand the time-varying coefficient functions in a time window with width  $\Delta T$ . Hence,

$$\Phi_i(t-i) = \sum_{l=0}^2 \mathbf{A}_{il}(t-i)^l = \tilde{\mathbf{A}}_i \mathbf{P}_i \quad \text{and} \quad \Theta_j(t-j) = \sum_{l=0}^2 \mathbf{B}_{il}(t-j)^l = \tilde{\mathbf{B}}_j \mathbf{T}_j, \quad (2)$$

where  $\mathbf{P}_i = \begin{bmatrix} [\mathbf{I}] & [\mathbf{I}](t-i) & [\mathbf{I}](t-i)^2 \end{bmatrix}^T$ ,  $\mathbf{T}_j = \begin{bmatrix} [\mathbf{I}] & [\mathbf{I}](t-j) & [\mathbf{I}](t-j)^2 \end{bmatrix}^T$ ,  $\tilde{\mathbf{A}}_i = [\mathbf{A}_{i0} \quad \mathbf{A}_{i1} \quad \mathbf{A}_{i2}]$  and  $\tilde{\mathbf{B}}_j = [\mathbf{B}_{j0} \quad \mathbf{B}_{j1} \quad \mathbf{B}_{j2}]$ . Substituting Eq. (2) into Eq. (1) and applying the continuous Cauchy wavelet transform (CCWT) to the resulting equation yield

$$W_{\psi_n}(a,b)\{\mathbf{z}(t)\} = \sum_{i=1}^I \tilde{\mathbf{A}}_i \Gamma_{b,i} + \sum_{j=0}^J \tilde{\mathbf{B}}_j \Omega_{b,j} + W_{\psi_n}(a,b)\{\bar{\mathbf{a}}(t)\}, \quad (3)$$

where

$$\Gamma_{b,i} = \begin{bmatrix} (W_{\psi_n}(a,b-i)\{\mathbf{z}(t)\}) \\ \left( \sum_{p=0}^1 C_p^1 (-ai)^p (b-i+ai)^{1-p} W_{\psi_{n-p}}(a,b-i)\{\mathbf{z}(t)\} \right) \\ \left( \sum_{p=0}^2 C_p^2 (-ai)^p (b-i+ai)^{2-p} W_{\psi_{n-p}}(a,b-i)\{\mathbf{z}(t)\} \right) \end{bmatrix}, \quad \Omega_{b,j} = \begin{bmatrix} (W_{\psi_n}(a,b-j)\{\bar{\mathbf{f}}(t)\}) \\ \left( \sum_{p=0}^1 C_p^1 (-ai)^p (b-j+ai)^{1-p} W_{\psi_{n-p}}(a,b-j)\{\bar{\mathbf{f}}(t)\} \right) \\ \left( \sum_{p=0}^2 C_p^2 (-ai)^p (b-j+ai)^{2-p} W_{\psi_{n-p}}(a,b-j)\{\bar{\mathbf{f}}(t)\} \right) \end{bmatrix};$$

the Cauchy continuous wavelet transform of a function of time,  $f(t)$ , is defined as [25]

$$W_{\psi_n}(a,b)\{f(t)\} = |a|^{-1/2} \int_{-\infty}^{\infty} f(t) \psi_n^* \left( \frac{t-b}{a} \right) dt; \quad (4)$$

the superscript\* denotes the complex conjugate;  $a$  is a dilation or scale parameter;  $b$  is a translation parameter, and  $\psi_n(t)$  is the Cauchy wavelet function and defined as [26]

$$\psi_n(t) = \left( \frac{i}{t+i} \right)^{n+1}; \quad (5)$$

$i = \sqrt{-1}$ . Notably, relations between the CCWTs of a function and its derivatives, relations between the CCWTs of  $f(t)$  and  $t^p f(t)$  and the translation-invariance property are used in developing Eq. (3).

The continuous wavelet transform in Eq. (4) shows its excellent ability of filtering  $f(t)$  in frequency domain. The frequency range is determined by the mother wavelet function and the chosen scale parameter. If only one value of  $a$  is used to establish Eq.(3), the responses  $\mathbf{z}(t)$  and input  $\mathbf{f}(t)$  within a certain frequency range



are used to find the time varying coefficients in the TVARX model. For considering a wide frequency range of responses  $\mathbf{z}(t)$  and input  $\mathbf{f}(t)$ , several values of  $a$  can be entered in Eq.(3).

Constructing Eq. (3) with different  $b$  and  $a$  (if necessary), whose corresponding time windows of Cauchy wavelets should be inside the time window of expanding time dependent coefficients under consideration by piecewise second-order polynomials, yields an over-determined system of linear algebraic equations. Applying the conventional least-squares approach to those linear algebraic equations and treating  $W_{\psi_n}(a,b)\{\bar{\mathbf{a}}(t)\}$  as error terms give the solutions for  $\tilde{\mathbf{A}}_i$  and  $\tilde{\mathbf{B}}_i$ . Then, the time dependent coefficient matrices  $\Phi_i(t)$  are obtained from Eq.(2). Similar to the procedure of obtaining modal parameters from an ARX model [27], a matrix  $[\mathbf{G}]$  is constructed from  $\Phi_i(t)$  as follows:

$$[\mathbf{G}] = \begin{bmatrix} [\mathbf{0}] & [\mathbf{I}] & [\mathbf{0}] & [\mathbf{0}] & \cdots & [\mathbf{0}] \\ [\mathbf{0}] & [\mathbf{0}] & [\mathbf{I}] & [\mathbf{0}] & \cdots & [\mathbf{0}] \\ \vdots & \vdots & \vdots & \vdots & \vdots & \vdots \\ [\mathbf{0}] & [\mathbf{0}] & [\mathbf{0}] & [\mathbf{0}] & \cdots & [\mathbf{I}] \\ \Phi_{I-1} & \Phi_{I-2} & \Phi_{I-3} & \cdots & \Phi_1 & \end{bmatrix}, \quad (6)$$

where  $[\mathbf{I}]$  is an  $2l \times 2l$  unit matrix;  $2l$  is the number of dimensions of  $\mathbf{z}(t)$  in Eq. (1). Instantaneous modal parameters (natural frequencies, damping ratios and mode shapes) of the structure can then be estimated from the time dependent eigenvalues and eigenvectors of  $[\mathbf{G}]$ .

## 2.2 Estimation of instantaneous stiffness matrices

Assuming that the mass matrix of a building,  $\mathbf{M}$ , is known and using a Bayesian methodology, Yuen [22] developed an objective function,  $J(\hat{\Omega}, \hat{\Psi}, \hat{\Delta})$ , to estimate the stiffness matrix of the structure using some of the identified natural frequencies and mode shapes of the building. The objective function is defined as

$$J(\hat{\Omega}, \hat{\Psi}, \hat{\Delta}) = \frac{1}{2} (\hat{\Delta} - \hat{\Delta}_\eta)^T \Sigma_{\hat{\Delta}}^{-1} (\hat{\Delta} - \hat{\Delta}_\eta) + \frac{1}{2\sigma_{eq}^2} \sum_{m=1}^{N_m} \left\| (\mathbf{K}(\hat{\Delta}) - \hat{\lambda}_m^2 \mathbf{M}) \hat{\psi}_m \right\|^2 + \frac{1}{2} \begin{bmatrix} \bar{\Omega} - \hat{\Omega} \\ \bar{\Psi} - \mathbf{L}_0 \hat{\Psi} \end{bmatrix}^T \Sigma_{\varepsilon}^{-1} \begin{bmatrix} \bar{\Omega} - \hat{\Omega} \\ \bar{\Psi} - \mathbf{L}_0 \hat{\Psi} \end{bmatrix} \quad (7)$$

where  $\bar{\Omega} = (\bar{\lambda}_1 \quad \bar{\lambda}_2 \quad \cdots \quad \bar{\lambda}_{N_m})^T$  ;  $\bar{\Psi} = (\bar{\psi}_1^T \quad \bar{\psi}_2^T \quad \cdots \quad \bar{\psi}_{N_m}^T)^T$  ;  $\hat{\Omega} = (\hat{\lambda}_1 \quad \hat{\lambda}_2 \quad \cdots \quad \hat{\lambda}_{N_m})^T$  ;  $\hat{\Psi} = (\hat{\psi}_1^T \quad \hat{\psi}_2^T \quad \cdots \quad \hat{\psi}_{N_m}^T)^T$  ;  $\bar{\lambda}_i$  and  $\hat{\lambda}_i$  are the identified and true angular frequencies of  $i^{\text{th}}$  mode, respectively;  $\bar{\psi}_i$  and  $\hat{\psi}_i$  are the identified and true  $i^{\text{th}}$  mode shapes, respectively;  $\hat{\Delta}$  is a vector including the unknown components to be determined in the stiffness matrix  $\mathbf{K}$ ;  $\hat{\Delta}_\eta$  is a vector of the nominal values of  $\hat{\Delta}$ ;  $\sigma_{eq}^2$  is a prescribed equation-error variance;  $\Sigma_{\hat{\Delta}}$  is the prior covariance matrix for  $\hat{\Delta}$ ;  $\Sigma_{\varepsilon}$  is the covariance matrix for  $((\bar{\Omega}^T, \bar{\Psi}^T) - (\hat{\Omega}^T, (\mathbf{L}_0 \hat{\Psi})^T))^T$ , and  $\mathbf{L}_0$  is an observation matrix that picks the components of  $\hat{\Psi}$  corresponding to the measured degrees of freedom. In the following analyses,  $\sigma_{eq}^2$  is set to 0.1%;  $\Sigma_{\hat{\Delta}}$  is a diagonal matrix with components equal to  $10^{-4}$ ;  $\Sigma_{\varepsilon}$  is also a diagonal matrix with the component corresponding to  $i^{\text{th}}$  mode equal to  $\bar{\lambda}_i \sigma_{eq}^2$ .



To determine  $\hat{\Psi}$ ,  $\hat{\Omega}$  and  $\hat{\Delta}$ , one carries out a sequence of iterations for the following optimization problems:

$$\Psi^* = \arg \min_{\Psi} J(\Omega^*, \hat{\Psi}, \Delta^*), \quad (8a)$$

$$\Omega^* = \arg \min_{\Omega} J(\hat{\Omega}, \Psi^*, \Delta^*), \quad (8b)$$

$$\Delta^* = \arg \min_{\Delta} J(\Omega^*, \Psi^*, \hat{\Delta}). \quad (8c)$$

The iteration starts from setting  $\Delta^* = \hat{\Delta}_\eta$  and  $\Omega^* = \bar{\Omega}$  to solve Eq. (8a), and sequentially Eqs. (8b) and (8c). The iteration process stops when  $\Delta^*$  converges.

### 3. Numerical simulation

Numerical simulation responses for a six-story shear building with time dependent material properties at the first story were first processed to confirm the accuracy and effectiveness of the proposed approach in determining instantaneous stiffness matrices of the building. The material properties of the six-story shear building are

$$m_i = 0.2 \text{ ton} \quad \text{for } i = 1 \sim 6 \quad (9a)$$

$$\left\{ \begin{array}{ll} c_1 = 300 \text{ N} \cdot \text{s} / \text{m} & 0 \leq t \leq 10 \text{ s} \\ c_1 = 300 \left[ 1 + 0.1 \sin \left( \frac{\pi(t-10)}{5} \right) \right] \text{ N} \cdot \text{s} / \text{m} & 10 \text{ s} < t \\ c_i = 300 \text{ N} \cdot \text{s} / \text{m} & (\text{for } i=2 \sim 6) \end{array} \right. \quad (9b)$$

$$\left\{ \begin{array}{ll} k_1 = 80 \text{ kN} / \text{m} & 0 \leq t \leq 10 \text{ s} \\ k_1 = 80 \left[ 1 - 0.1 \sin \left( \frac{\pi(t-10)}{5} \right) \right] \text{ kN} / \text{m} & 10 \text{ s} < t \\ k_i = 80 \text{ kN} / \text{m} & (\text{for } i=2 \sim 6) \end{array} \right. \quad (9c)$$

where  $m_i$ ,  $c_i$  and  $k_i$  denote the mass, damping coefficient and stiffness of the  $i^{\text{th}}$  floor or story, respectively.

The Runge-Kutta method was applied to solve the equations of motion for the shear building with a time increment ( $\Delta t$ ) of 0.004 s. Figure 1 shows the time histories of base excitation and acceleration responses at the first, second and sixth floors. These responses and input adding white noise with NSR=10% for  $5 \leq t \leq 35$  s are processed.

Figure 2 displays the variations of instantaneous natural frequencies of the six modes with time. Those instantaneous frequencies are identified following the procedure given in section 2.1 with  $\Delta T = 2$  s and using Cauchy wavelets with  $n=10$ . Scale factors  $a=2, 0.75, 0.46, 0.35, 0.3$  and  $0.27$  are used to identify modal parameters of modes 1~6, respectively. The figure demonstrates that the identified natural frequencies agree excellently with the true values with the differences less than 1.5%. The identified mode shapes, which are not shown here, are also consistent with the true ones with MAC larger than 0.98.

When applying the procedure shown in section 2.2 to determine the stiffness matrix of a building using the identified modal parameters, one has to know the structure of the stiffness matrix. That is, the bandwidth of the

stiffness matrix ( $B_w$ ) must be first determined for the problem under consideration herein. The bandwidth of  $K$  for a shear building is one. However, different bandwidths of  $K$  are chosen to approximate the stiffness matrix at  $t=17.5$  s, and the results are listed in Table 1. As  $B_w$  increases, more stiffness components are to be identified. For example, when  $B_w$  is set to three, there are 18 components in  $K$  to be determined with the assumption of a symmetric  $K$ .

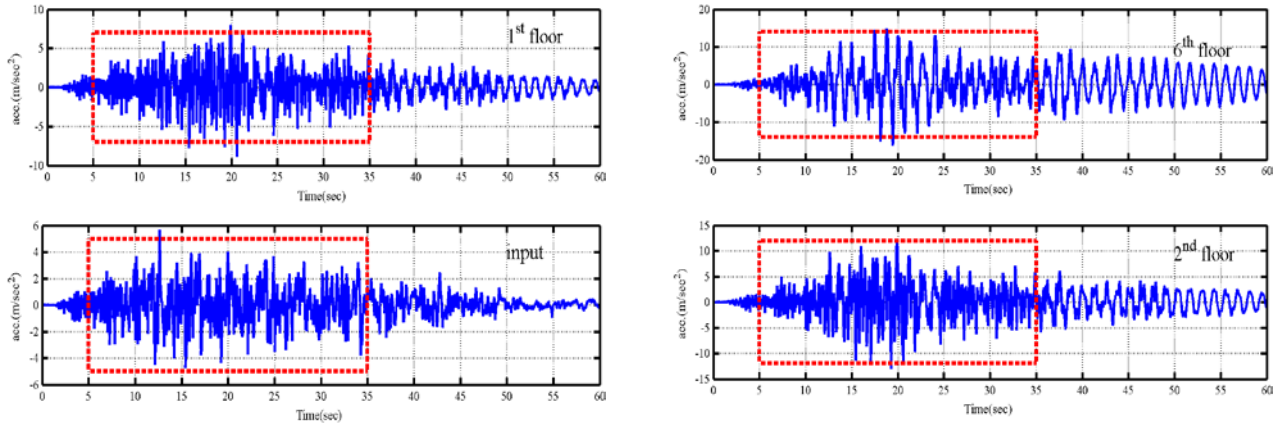


Fig.1 Time histories of input and acceleration responses

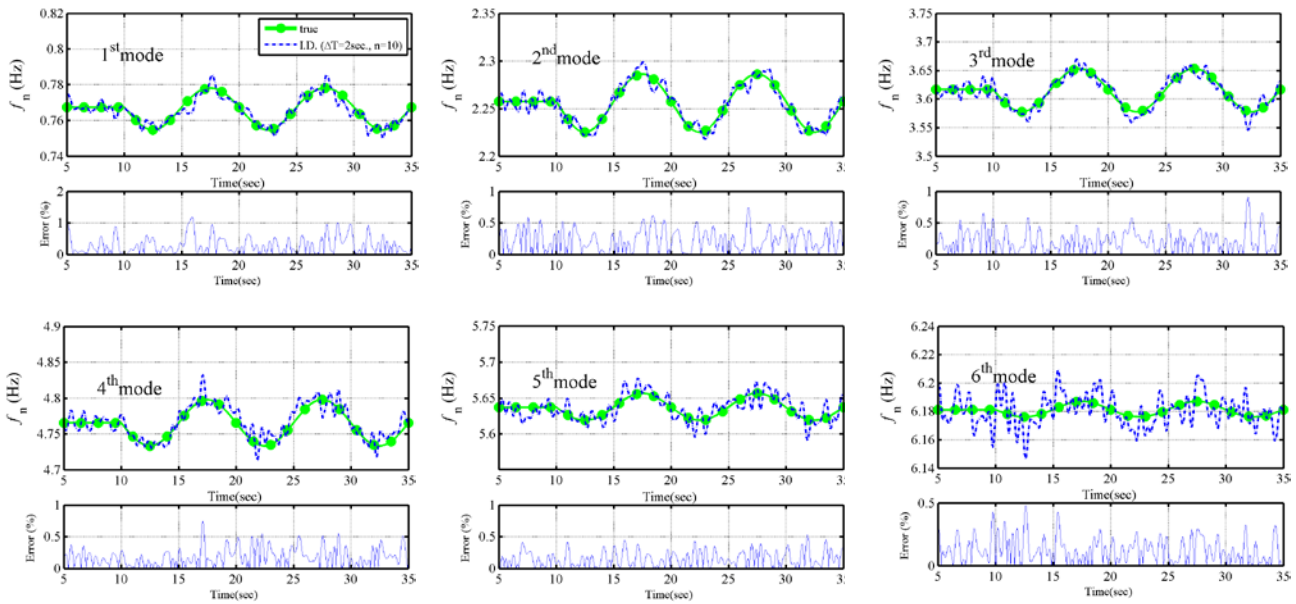


Fig. 2 Identified instantaneous natural frequencies

The results in Table 1 are obtained using the identified modal parameters of the first three modes. The other identified modal parameters are employed to verify the correctness of the chosen bandwidths of matrix. The nominal values for the stiffness components, which are needed in  $\hat{\Delta}_\eta$ , are set as follows:  $k_{ij,\eta} = 1.3 k_{ij,true}$  for  $j=i$  and  $i+1$ ,  $k_{i(i+2),\eta} = 10$  kN/m and  $k_{i(i+3),\eta} = 1$  kN/m, where subscript ‘true’ indicates the true values. The nominal values for the stiffness components can be estimated from the design data of the building under consideration. It is reasonable to assume that the differences between the nominal values and true values are less than 30%. The values of  $k_{ij}$  with  $j \geq i+2$  or  $j \leq i-2$  theoretically equal zero, and it is also reasonable to set small nominal values for those components. The parenthesized values in Table 1 indicate the relative errors of the identified results, and clearly show that if the assumed  $B_w$  is more different from the true one, the worse



results are identified. The relative errors of the stiffness components identified by assuming  $B_w=3$  can reach more than 70%, while the relative errors for  $B_w=2$  are less than 30%. When  $B_w=1$  (the true value), the identified results are very accurate with the relative errors less than 1%.

Table 1 Identified stiffness matrices at  $t=17.5$  s by assuming different bandwidths of matrix

Bandwidth ( $B_w$ )	Identified $\mathbf{K}$ (kN/m)
3	$\begin{bmatrix} 93.48 (16.9\%) & -105.12 (31.4\%) & 13.74 & 0.01 & 0 & 0 \\ -105.12 & 201.73 (26.1\%) & -119.00 (48.7\%) & 19.01 & 0.03 & 0 \\ 13.74 & -119.00 & 203.09 (26.9\%) & -112.11 (40.1\%) & 14.75 & 0.00 \\ 0.01 & 19.01 & -112.11 & 198.07 (23.8\%) & -111.63 (39.5\%) & 20.29 \\ 0 & 0.03 & 14.75 & -111.63 & 206.80 (29.3\%) & -110.19 (37.7\%) \\ 0 & 0 & 0.00 & 20.29 & -110.19 & 200.40 (19.3\%) \end{bmatrix}$
2	$\begin{bmatrix} 89.29 (11.6\%) & -94.44 (18.1\%) & 8.14 & 0 & 0 & 0 \\ -94.44 & 187.54 (17.2\%) & -101.42 (26.8\%) & 5.60 & 0 & 0 \\ 8.14 & -101.42 & 182.25 (13.9\%) & -96.20 (20.3\%) & 4.43 & 0 \\ 0 & 5.60 & -96.20 & 177.38 (10.9\%) & -86.08 (7.60\%) & 0.21 \\ 0 & 0 & 4.43 & -86.08 & 163.71 (2.32\%) & -79.51 (0.61\%) \\ 0 & 0 & 0 & 0.21 & -79.51 & 167.81 (0.11\%) \end{bmatrix}$
1	$\begin{bmatrix} 80.54 (0.68\%) & -80.21 (0.26\%) & 0 & 0 & 0 & 0 \\ -80.21 & 160.02 (0.01\%) & -80.36 (0.45\%) & 0 & 0 & 0 \\ 0 & -80.36 & 160.49 (0.31\%) & -80.23 (0.29\%) & 0 & 0 \\ 0 & 0 & -80.23 & 159.90 (0.06\%) & -79.72 (0.35\%) & 0 \\ 0 & 0 & 0 & -79.72 & 160.33 (0.20\%) & -79.90 (0.12\%) \\ 0 & 0 & 0 & 0 & -79.90 & 168.27 (0.16\%) \end{bmatrix}$

A question arises how to determine a right  $B_w$ . Table 2 shows the comparisons between modal parameters obtained from TVARX models and those determined from the stiffness matrices in Table 1. The index proposed by Trifunac [28] is adopted to indicate the correlation between two mode shapes and is defined as

$$e = \left( \frac{(\boldsymbol{\Psi}_{iT} - \alpha \boldsymbol{\Psi}_{iI})^T (\boldsymbol{\Psi}_{iT} - \alpha \boldsymbol{\Psi}_{iI})}{(\boldsymbol{\Psi}_{iT})^T (\boldsymbol{\Psi}_{iT})} \right)^{1/2}, \quad (10)$$

where  $\boldsymbol{\Psi}_{iI}$  and  $\boldsymbol{\Psi}_{iT}$  represent mode shapes obtained from a TVARX model and a stiffness matrix, respectively, and  $\alpha$  is determined by minimizing  $(\boldsymbol{\Psi}_{iT} - \alpha \boldsymbol{\Psi}_{iI})^T (\boldsymbol{\Psi}_{iT} - \alpha \boldsymbol{\Psi}_{iI})$ . When  $e$  is close to zero, the two mode shapes are highly correlated. Table 2 reveals that the natural frequencies and mode shapes of the first three modes determined from the identified stiffness matrices with  $B_w=1$  and 2 are consistent with those identified from TVARX models. The modal parameters of the 4<sup>th</sup> to 6<sup>th</sup> modes determined from the stiffness matrices with wrong  $B_w$  are significantly different from those of TVARX models. Consequently, the identified modal parameters that are not applied to establish a stiffness matrix are useful to determine the right bandwidth of the wanted stiffness matrix.

Table 3 summarizes the identified stiffness matrices at  $t=7.5$  s, 12.5 s and 17.5 s by setting  $B_w=1$ . The results are consistent with the true ones and clearly reveal that only  $k_{66}$  at these matrices are significantly different from each other, while the other components only slightly change. It indicates that the changes of story stiffness happen at the first story, and the amount of changes is easily found.

Table 2 Comparisons between modal parameters obtained from TVARX models and identified stiffness matrices

Bandwidth (B <sub>w</sub> )	Modal parameters	Mode					
		1	2	3	4	5	6
3	$f_n$ (Hz)	0.78	2.30	3.66	5.03	6.44	7.33
	$e$	0.29	0.18	0.04	0.04	0.02	0.04
2	$f_n$ (Hz)	0.78	2.30	3.66	4.94	5.87	6.67
	$e$	0.00	0.00	0.01	0.14	0.10	0.33
1	$f_n$ (Hz)	0.78	2.30	3.66	4.80	5.66	6.19
	$e$	0.00	0.00	0.00	0.00	0.00	0.01
TVARX	$f_n$ (Hz)	0.78	2.30	3.66	4.79	5.66	6.19

Table 3 Identified stiffness matrices at different time by assuming B<sub>w</sub>=1

$t$ (s)	Identified <b>K</b> (kN/m)		
7.5	$\begin{bmatrix} 80.22 & -80.10 & 0 & 0 & 0 & 0 \\ -80.10 & 159.73 & -80.03 & 0 & 0 & 0 \\ 0 & -80.03 & 160.43 & -79.91 & 0 & 0 \\ 0 & 0 & -79.91 & 159.76 & -80.30 & 0 \\ 0 & 0 & 0 & -80.30 & 160.85 & -80.44 \\ 0 & 0 & 0 & 0 & -80.44 & 160.69 \end{bmatrix}$		
	12.5	$\begin{bmatrix} 80.07 & -79.85 & 0 & 0 & 0 & 0 \\ -79.85 & 159.37 & -79.80 & 0 & 0 & 0 \\ 0 & -79.80 & 159.88 & -79.65 & 0 & 0 \\ 0 & 0 & -79.65 & 159.30 & -79.94 & 0 \\ 0 & 0 & 0 & -79.94 & 160.26 & -80.11 \\ 0 & 0 & 0 & 0 & -80.11 & 152.17 \end{bmatrix}$	
		17.5	$\begin{bmatrix} 80.54 & -80.21 & 0 & 0 & 0 & 0 \\ -80.21 & 160.02 & -80.36 & 0 & 0 & 0 \\ 0 & -80.36 & 160.49 & -80.23 & 0 & 0 \\ 0 & 0 & -80.23 & 159.90 & -79.72 & 0 \\ 0 & 0 & 0 & -79.72 & 160.33 & -79.90 \\ 0 & 0 & 0 & 0 & -79.90 & 168.27 \end{bmatrix}$



Fig. 3 A photo of five-story steel frame

#### 4. Application to a steel frame in shaking table tests

Shaking table tests are often performed in a laboratory to examine the behavior of structures in earthquakes. A series of shaking table tests were carried out on a five-story steel frame with 3 m long, 2 m wide and 6.5 m high (see Fig. 3). Lead blocks were piled on each floor such that the mass of each floor was approximately 3664 kg. The dynamic responses of the frame under the base excitation of 60% of the strength the Kobe earthquake in the long span direction are considered herein. Measured strains and visual inspection revealed yielding of the steel columns near the first floor. Figure 4 depicts time histories of input base excitation and the acceleration responses of 1<sup>st</sup>, 3<sup>rd</sup> and 5<sup>th</sup> floors.

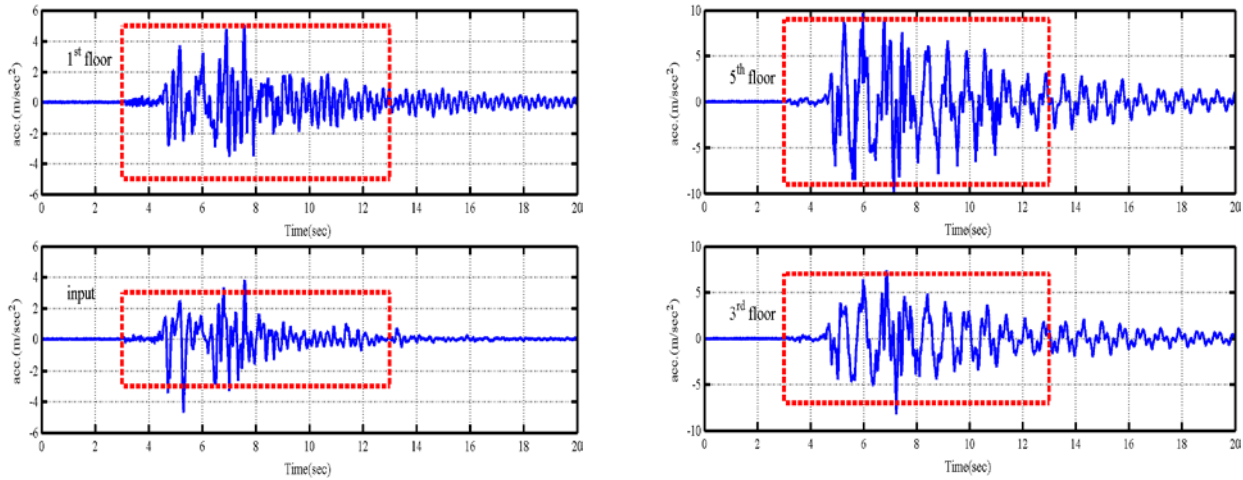


Fig.4 Time histories of input and acceleration responses of 1<sup>st</sup>, 3<sup>rd</sup> and 5<sup>th</sup> floors in the shaking table test

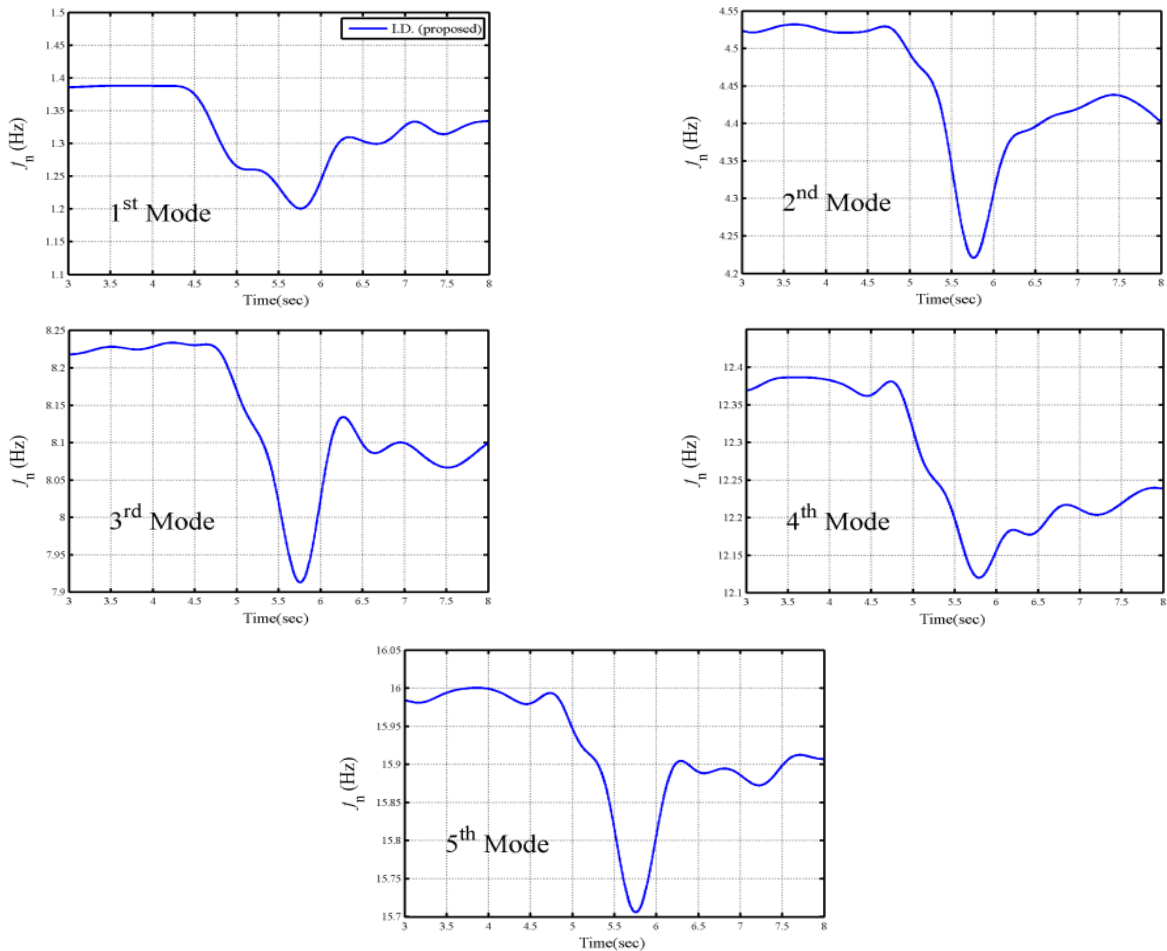


Fig. 5 Identified instantaneous natural frequencies of a five-story steel frame

Using input base excitation and the responses for  $3 \text{ s} \leq t \leq 13 \text{ s}$  of all the floors and following the procedure of identifying instantaneous modal parameters given in section 2, one obtains the variations of the instantaneous natural frequencies of five modes with time shown in Fig. 5. The details for determining these results are given in [23]. Figure 5 reveals that the variations of the identified natural frequencies over time are less than 2% at  $t \leq 4.5 \text{ s}$ , and a significant decrease of the natural frequencies begins around  $t=5 \text{ s}$ . The



considerable decrease of the natural frequencies strongly indicates that some of the steel columns of the frame started to yield around that moment.

To investigate the decrease of stiffness caused by yielding, the stiffness matrices of the frame at  $t=4$  s and 5.76 s are estimated using the identified modal parameters of the first four modes at these two particular time by following the same procedure described above. The floors are assumed rigid, which is a typical assumption used in a design process. Because the frame is symmetric, the frame can be treated as a five degrees of freedom system when it is subjected to base excitation in its long span direction. The modal components of the first five modes are listed in Table 4. The estimated stiffness matrices are given in Table 5. The bandwidths of the best-fit stiffness matrices are three, which indicates that the steel frame does not completely behave like a shear building. Comparing the components of stiffness matrices before and after yielding of columns reveals that the maximum change in the diagonal components happens at component (5,5) and the relative difference is about 7.3%, while the relative differences for other diagonal components are less than 4%. Consequently, the columns of the first story were the most likely to yield during the shaking table test, which is consistent with what is found from the measured strains.

Table 4 Identified modal components of five modes

Floor	$t=4$ s					$t=5.76$ s				
	Mode					Mode				
	1	2	3	4	5	1	2	3	4	5
5	1.00	-0.94	0.97	-0.46	-0.21	1.00	-0.93	0.96	-0.48	-0.14
4	0.90	-0.16	-0.94	1.00	0.68	0.90	-0.17	-0.86	1.00	0.70
3	0.69	0.65	-0.98	-0.51	-0.96	0.72	0.67	-0.99	-0.45	-0.99
2	0.47	1.00	0.77	-0.51	1.00	0.49	1.00	0.71	-0.56	1.00
1	0.17	0.48	1.00	0.85	-0.65	0.17	0.49	1.00	0.82	-0.66

Table 5 Identified stiffness matrices (unit: kN/m)

$t=4$ s	$t=5.76$ s
$\begin{bmatrix} 5173.7 & -6721.9 & 1655.7 & 0 & 0 \\ -6721.9 & 14217.8 & -9244.3 & 1527.9 & 0 \\ 1655.7 & -9244.3 & 15184.7 & -9023.9 & 1719.3 \\ 0 & 1527.9 & -9023.9 & 15273.1 & -10229.0 \\ 0 & 0 & 1719.3 & -10229.0 & 18174.9 \end{bmatrix}$	$\begin{bmatrix} 5016.0 & -6702.2 & 1761.7 & 0 & 0 \\ -6702.2 & 13903.1 & -9114.4 & 1648.1 & 0 \\ 1761.7 & -9114.4 & 14612.5 & -8827.3 & 1908.9 \\ 0 & 1648.1 & -8827.3 & 14719.8 & -9944.2 \\ 0 & 0 & 1908.9 & -9944.2 & 16848.9 \end{bmatrix}$

## 5. Concluding remarks

The work proposed an approach for assessing damage in a building under a strong earthquake by using its acceleration responses under such earthquake. The data of a building without damage is not needed, and the effects of environmental conditions such as temperature and humidity can be neglected. The measured acceleration responses of a building and the input excitation are used to determine its instantaneous modal parameters through establishing an appropriate TVARX model. The time-varying coefficient matrices in a TVARX model are expanded using piecewise second order polynomials. The Cauchy wavelet transforms with proper scale parameters and translation parameters are employed to the TVARX model to determine the time-varying coefficient matrices. The instantaneous modal parameters are obtained from the identified coefficients of AR. The stiffness matrices of the building varying with time are estimated using those identified instantaneous



modal parameters through a Bayesian model updating procedure. The damage assessment is carried out by comparing the stiffness components at different particular time in an earthquake.

The proposed approach was validated first by processing the numerically simulated acceleration responses of a six-story shear building with time dependent stiffness and damping in the first story. The responses of three floors and input excitation with 10% random noise were processed to accurately identify the instantaneous modal parameters of six modes. The identified instantaneous modal parameters of the first three modes were employed to determine the instantaneous stiffness matrices via the Bayesian model updating procedure of Yuen [22]. The instantaneous modal parameters of the other modes were used to determine an appropriate bandwidth of stiffness matrix. The instantaneous stiffness matrices were accurately identified.

The proposed approach was further applied to assess damage of a five-story steel frame in a shaking table test with the input of 60% of the strength the Kobe earthquake. The acceleration responses of all floors were used to identify the instantaneous modal parameters of five modes. Significant changes in the instantaneous natural frequencies were observed. The instantaneous modal parameters of the first four modes before and just after the significant decreases in frequencies were used to establish the corresponding stiffness matrices, which show that the maximum change of stiffness occurs at the first story. The findings from the analyses are consistent with what are observed from the measured strains.

## 6. Acknowledgements

The authors would like to thank the Ministry of Science and Technology of the Republic of China, Taiwan, for financially supporting this research under Contract No. MOST 104-2221-E-009-131. The appreciation is also extended to the National Center for Research on Earthquake Engineering for providing shaking table test data.

## 7. References

- [1] Mottershead JE, Friswell MI (1993): Model updating in structural dynamics. *Journal of Sound and Vibration* 167(2), 347-375.
- [2] Salawu OS (1997): Detection of structural damage through changes in frequency: a review. *Engineering Structures* 19(9), 718-723.
- [3] Farrar CR, Doebling SW, Nix DA (2001): Vibration-based structural damage identification. *Philosophical Transactions of the Royal Society A; Mathematical, Physical and Engineering Science* 359(1778), 131-150.
- [4] Chang PC, Flatau A, Liu SC (2003): Review paper: health monitoring of civil infrastructure. *Structural Health Monitoring, An International Journal* 2(3), 257-267.
- [5] Friswell MI, Penny JET, Wilson DAL (1994): Using vibration data and statistical measures to locate damage in structures. *The International Journal of Analytical and Experimental Modal Analysis* 9(4), 239-254.
- [6] Messina A, Williams EJ, Contursi T (1998): Structural damage detection by a sensitivity and statistical-based method. *Journal of Sound and Vibration* 216(5), 791-808.
- [7] Zapico JL, González MP (2003): Damage assessment using neural networks. *Mechanical System and Signal Processing* 17(1), 119-125.
- [8] Allemang RJ, Brown DL (1983): A correlation coefficient for modal vector analysis. *1<sup>st</sup> International Modal Analysis Conference*, Bethel, Connecticut, USA.
- [9] Lieven NAJ, Ewins DJ (1988): Spatial correlation of mode shapes, the coordinate modal assurance criterion (COMAC). *6<sup>th</sup> International Modal Analysis Conference*, Kissimmee, Florida, USA.
- [10] Chen JC, Garba JA (1988): On-orbit damage assessment for large space structures. *AIAA Journal* 26(9), 1119-1126.
- [11] Law SS, Shi ZY, Zhang LM (1998): Structural damage detection from incomplete and noisy modal test data. *Journal of Engineering Mechanics, ASCE* 124(11), 1280-1288.
- [12] Shi ZY, Law SS, Zhang LM (1998): Structural damage location from modal strain energy change. *Journal of Sound and Vibration* 218(5), 825-844.



- [13] Pandey AK, Biswas M, Samman MM (1991): Damage detection from changes in curvature mode shapes. *Journal of Sound and Vibration* 145(2), 321-332.
- [14] Sampaio RPC, Maia NMM, Silva JMM (1999): Damage detection using the frequency-response-function curvature method. *Journal of Sound and Vibration* 226(5), 1029-1042.
- [15] Lin CS (1990): Location of modeling errors using modal test data. *AIAA Journal* 28(9), 1650-1654.
- [16] Pandey AK, Biswas M (1994): Damage detection in structures using changes in flexibility. *Journal of Sound and Vibration* 169(1), 3-17.
- [17] Koh CG, See LM, Balendra T (1991): Estimation of structural parameters in the time domain: a substructure approach. *Earthquake Engineering and Structural Dynamics* 20(8), 787-801.
- [18] Zhao Q, Sawada T, Hirao K, Nariyuki Y (1995): Localized identification of MDOF structures in the frequency domain. *Earthquake Engineering and Structural Dynamics* 24(3), 325-338.
- [19] Su WC, Huang CS, Hung SL, Chen LJ, Lin WJ (2012): Locating damaged storeys in a shear building based on its sub-structural natural frequencies. *Engineering Structures* 39(1), 126-138.
- [20] Moser P, Moaveni B (2011): Environmental Effects on the Identified Natural Frequencies of the Dowling Hall Footbridge. *Mechanical System and Signal Processing* 25(7), 2336-2357.
- [21] Wood MG (1992): *Damage Analysis of Bridge Structures Using Vibration Techniques*, Ph. D dissertation, University of Aston, Birmingham, Birmingham, UK.
- [22] Yuen KV (2010): *Bayesian Methods for Structural Dynamics and Civil Engineering*. John Wiley & Sons Pte Ltd.
- [23] Huang CS, Liu CY, Su WC (2016): Application of Cauchy wavelet transformation to identify time-variant modal parameters of structures. *Mechanical System and Signal Processing* 80(1), 302-323.
- [24] Huang CS, Hung SL, Su WC, Wu CL (2009): Identification of time-variant modal parameters using TVARX and low-order polynomial function. *Computer-Aided Civil and Infrastructure Engineering* 24(7), 470-491.
- [25] Chui CK (1992): *An Introduction to Wavelets, Wavelet Analysis and its Application volume 1*, Academic Press, Boston.
- [26] Argoul P, Le TP (2003): Instantaneous indicators of structural behavior based on the continuous cauchy wavelet analysis. *Mechanical System and Signal Processing* 17 (1), 243-250.
- [27] Huang CS (2001): Structural identification from ambient vibration measurement using the multivariate AR model. *Journal of Sound and Vibration* 241 (3), 337-359.
- [28] Trifunac D (1972): Comparisons between ambient and forced vibration experiments. *Earthquake Engineering and Structural Dynamics* 1, 133-150 .